

## THEORETICAL STUDIES ON THE STRUCTURE AND SPECTROSCOPIC PROPERTIES OF PSEUDOHALIDES

N. B. Okulik,<sup>1</sup> A. H. Jubert,<sup>2</sup> and E. A. Castro<sup>3</sup>

UDC 544.15;544.18;543.42

Pseudohalogen-containing compounds have attracted significant interest among nonmetal chemists and theorists, not only owing to their potential use in various fields but also due to difficulties in their experimental preparation and characterization. Since its introduction in 1925, the pseudohalide principle has been used extensively and, therefore, a remarkable progress has been made in the experimental and theoretical research on the compounds of this kind. In this work, we review studies on structural investigations and theoretical characterizations of several pseudohalide-containing compounds in order to contribute to better understanding of the chemistry of many such species.

**Keywords:** pseudohalides, photoelectron spectroscopy, theoretical calculations, DFT, *ab initio* methods.

### LIST OF ABBREVIATIONS USED

AIM	atoms in molecules
B3P86	Becke's three parameter hybrid functional with Perdew 86
B3LYP	Becke's three parameter hybrid functional using the LYP correlation functional
B3PW91	Becke's three parameter hybrid functional with Perdew/Wang 91
CCSD(T)	coupled-cluster theory with singles, doubles, and noniterative approximation of triples
CI	configuration interaction
DFT	density functional theory
ECP	effective core potential
GVB	generalized valence bond
HF	Hartree–Fock
HOMO	highest occupied molecular orbital
IE	ionization energy
IP	ionization potential
LUMO	lowest unoccupied molecular orbital
MO	molecular orbital theory
MP2	Möller–Plesset perturbation theory terminated at second order
MP3	Möller–Plesset perturbation theory terminated at third order

---

<sup>1</sup>Facultad de Agroindustrias, Universidad Nacional del Nordeste, R.S. Peña, Chaco, Argentina. <sup>2</sup>Programa CEQUINOR, Departamento de Química, Facultad de Ciencias Exactas, UNLP, Calle 47 y 115, La Plata 1900, Buenos Aires, Argentina. <sup>3</sup>INIFTA (CCT-LP, CONICET-UNLP), División Química Teórica, Departamento de Química, Facultad de Ciencias Exactas, UNLP, Diag. 113 y 64, Suc. 4, C.C. 16, La Plata 1900, Buenos Aires, Argentina; eacast@gmail.com. The text was submitted by the authors in English. *Zhurnal Strukturnoi Khimii*, Vol. 49, No. 5, pp. 956-970, September-October, 2008. Original article submitted December 2, 2007; revised February 29, 2008.

MP4	Möller–Plesset perturbation theory terminated at fourth order
MP4SDQ	MP4 with single, double and quadruple substitutions
MP4SDTQ	MP4 with single, double, triple and quadruple substitutions
MPW1PW91	one parameter hybrid functional with modified Perdew–Wang exchange and correlation
OVGF	outer valence green function
PES	photoelectron spectroscopy
PIMS	photoionization mass spectra
QCISD(T)	quadratic configuration-interaction method, with triple substitutions
QCISD	quadratic configuration-interaction method, without triple substitutions
VB	valence-bond theory
ZPE	zero point of energy

## INTRODUCTION

The goal of the interpretative theoretical research is to present models which help to qualitatively understand and predict the structures and reactivities of molecules. Sophisticated quantum chemical methods have been developed for calculating measurable properties of molecules such as energies, geometries, vibrational frequencies, etc., as well as to analyze the calculated electronic structure aiming at providing a meaningful insight into the bonding situation of a molecule and building a bridge between the chemical behavior of the molecule and the underlying physical laws.

Quantum theory employed rather complicated mathematical formalism in order to explain the chemical bond, while chemists were trained to employ simple models and empirically derived rules for rationalizing molecular structures and chemical reactivity. So, the work of Hückel [1] in aromatic compounds was not adopted by chemists for several decades [2]. Linus Pauling was able to build a bridge between quantum chemistry and the empirically derived models which were commonly used by chemists [3]. He resorted to valence-bond (VB) theory, because the familiar model of a two-electron bond could easily be retained and introduced hybridization as a very helpful device to rationalize the geometries, bond energies, and other physical molecular properties.

To our knowledge, the importance of quantum chemistry in the field of pseudo- halide compounds was comparatively moderate until the end of the 1980s but at present the situation has changed due to the successful employment of gradient-corrected density functional theory (DFT) in calculating molecules, particularly for those molecular species containing heavier atoms [4]. DFT has proven to be very powerful because the Kohn-Sham orbitals turned out to be even more helpful for a bonding analysis in terms of orbital interactions than the Hartree–Fock (HF) orbitals, since the former include correlation effects. Thus, this methodology made it possible to calculate geometries, bond energies, vibrational spectra and analyze the chemical bonds of the molecules with the aim of gaining a deeper insight into the most significant features related to the chemical bond.

In this paper we want to discuss the progresses that has been made mainly in the past two decades toward a better understanding of the structure and bonding interactions in pseudohalide-containing compounds, focusing on quantum chemical studies utilized DFT or *ab initio* methods. We have selected those significant contributions which are based on structure determination if they are relevant to providing meaningful information about the nature of the chemical bond.

Pseudohalogens are compounds that resemble the halogen elements,  $X_2$ , in their chemistry, e.g.  $(CN)_2$  cyanogen,  $(SCN)_2$  thiocyanogen, ICN iodine cyanide. Certain ions that have sufficient resemblance to halide ions are sometimes referred to as pseudohalide ions, e.g.  $N_3^-$ ,  $SCN^-$ ,  $CN^-$  [5].

The pseudohalide concept was introduced in 1925 [6] and it has been used extensively in nonmetal chemistry to predict the molecular structure and chemical stability of various species. Ever since, outstanding progress has been made in

the experimental and theoretical research on pseudohalides, e.g. in compounds containing  $\text{CN}^-$ ,  $\text{OCN}^-$ ,  $\text{CNO}^-$ ,  $\text{SCN}^-$ ,  $\text{SeCN}^-$ ,  $\text{TeCN}^-$ ,  $\text{N}_3^-$  [7], posing new challenges for their preparation and providing better understanding of these species.

Due to their rich chemistry, pseudohalides are widely used as building blocks for polymers, synthetic precursors and key intermediates for biologically active compounds. Therefore, a great number of papers dealing with the coordination chemistry of pseudohalide anions [8-12] and numerous other structural studies about pseudohalide compounds which focus on accurate structural determinations and various properties such as geometries, vibrational frequencies, NMR chemical shifts, etc., have been published in the past decade [13]. Although these works are important for the understanding of the molecular behavior, they fall beyond the scope of this review and will not be discussed here.

### PHOTOELECTRON SPECTROSCOPY OF $\text{XN}_3$ ( $\text{X} = \text{Cl}, \text{Br}$ ), $\text{XNCO}$ , $\text{XSCN}$ , $\text{XSeCN}$ ( $\text{X} = \text{Cl}, \text{Br}, \text{I}$ ) AND CALCULATED STRUCTURE OF IODO DERIVATIVES

The photoelectron spectroscopy (PES) [14] technique can be used to identify and study short-lived molecules, such as pseudohalides, usually prepared by on-line methods. HeI photoelectron spectra of unstable halogen azides,  $\text{XN}_3$  ( $\text{X} = \text{Cl}$  and  $\text{Br}$ ) and the halogen isocyanates,  $\text{XNCO}$  ( $\text{X} = \text{Cl}, \text{Br}$  and  $\text{I}$ ) were obtained [15] and the results were compared with *ab initio* and semi-empirical calculations. It was possible to reassign the photoelectron spectra of the parent acids,  $\text{HN}_3$  and  $\text{HNCO}$ , in the high energy region and that provided quite an interesting illustration of how the orbitals of a linear pseudohalide grouping are perturbed by an off-axis halogen atom. Other compounds, such as  $\text{XNCO}$ ,  $\text{XSCN}$ , and  $\text{XSeCN}$  ( $\text{X} = \text{Cl}, \text{Br}$ ), have been prepared in the gas phase by heterogeneous reactions of the chlorine gas or bromine vapor with corresponding silver salts  $\text{AgNCO}$ ,  $\text{AgSCN}$ , and  $\text{AgSeCN}$ ; the compounds also have been characterized on-line by PES in combination with sophisticated quantum chemical calculations [15]. Following a procedure analogous to the preparation of  $\text{BrNCO}$ , iodine isocyanate (INCO) and iodine thiocyanate (ISCN) were prepared and their PE spectra were recorded, although there were some byproducts showing in the spectra [16]. Further reports have been published on the preparation in the gas phase of pure  $\text{XN}_3$  ( $\text{X} = \text{F}, \text{Cl}, \text{Br}, \text{I}$ ) compounds and they were characterized on-line by PES technique combined with the outer valence green function (OVGF) calculations [17].

Furthermore, a procedure for preparing pure gas-phase INCO, ISCN and the hitherto unknown  $\text{ISeCN}$  was reported and the products also were characterized by PES technique in combination with OVGF calculations [18].

The geometries of INCO, ISCN, and  $\text{ISeCN}$  molecules were optimized at 6-311++G(2df,pd) basis set level with four different methods: B3P86, B3LYP, B3PW91, and MP2. Table 1 show that the agreement of the results in the geometry optimization using the four different methods is quite good for INCO, ISCN and  $\text{ISeCN}$ .

**TABLE 1.** Optimized Geometrical Structures of  $\text{ISeCN}$ ,  $\text{ISCN}$ , and  $\text{INCO}$  at 6-311++G(2df,pd) Basis Set Level with Four Different Methods<sup>a</sup>

Species		B3P86	B3LYP	B3PW91	MP2	Species		B3P86	B3LYP	B3PW91	MP2
ISeCN	$R_{\text{I-Se}}$	2.47	2.51	2.48	2.46	INCO	$\angle \text{ISC}$	100.9	101.3	100.9	99.3
	$R_{\text{Se-C}}$	1.83	1.84	1.83	1.82		$\angle \text{SCN}$	175.9	175.9	175.9	176.4
	$R_{\text{C-N}}$	1.15	1.16	1.16	1.18		$\angle \text{ISCN}$	180.0	180.0	180.0	180.0
	$\angle \text{ISeC}$	97.7	98.0	97.7	96.7		$R_{\text{I-N}}$	1.96	1.98	1.97	1.96
	$\angle \text{SeCN}$	177.2	177.0	177.1	177.6		$R_{\text{N-C}}$	1.21	1.21	1.21	1.22
	$\angle \text{ISeCN}$	180.0	180.0	180.0	180.0		$R_{\text{C-O}}$	1.16	1.16	1.16	1.17
ISCN	$R_{\text{I-S}}$	2.36	2.39	2.36	2.35	$\angle \text{INC}$	130.5	130.2	130.4	128.4	
	$R_{\text{S-C}}$	1.68	1.69	1.68	1.69	$\angle \text{NCO}$	173.6	173.7	173.6	173.0	
	$R_{\text{C-N}}$	1.16	1.16	1.16	1.18	$\angle \text{INCO}$	180.0	180.0	180.0	180.0	

<sup>a</sup>Taken from ref. [18]. Lengths ( $R$ ) in Å, angles ( $\angle$ ) in degrees.

**TABLE 2.** PES Ionization Energies (IP) and Computed Ionization Energies (Ev) by the OVGf Calculation with 6-311++G(2df) Basis Sets and Molecular Orbital-Ionized Character for SO(N<sub>3</sub>)<sub>2</sub><sup>a</sup>

IP (eV)	Ev (eV)	MO character	IP (eV)	Ev (eV)	MO character
10.18	10.244(33)	$\pi$ N <sub>6</sub> -N <sub>7</sub> -N <sub>8</sub> *	13.08	13.519(29)	$\sigma$ S-O*, $\sigma$ N <sub>3</sub> -N <sub>4</sub>
10.50	10.616(32)	$\pi$ N <sub>6</sub> -N <sub>7</sub> -N <sub>8</sub> *	13.59		
11.15	10.769(31)	$\pi$ N <sub>3</sub> -N <sub>4</sub> -N <sub>5</sub> *	14.94	14.226(28)	$\pi$ S-O, $\pi$ N <sub>7</sub> -N <sub>8</sub>
11.48	11.441(30)	$\pi$ N <sub>3</sub> -N <sub>4</sub> -N <sub>5</sub> *	15.69	15.163(27)	$\pi$ S-O, $\pi$ N <sub>4</sub> -N <sub>5</sub>

<sup>a</sup>Taken from ref. [ 19 ].

Due to the absence of experimental geometrical results, the calculations of the ionization energies using the OVGf method were carried out at the 6-311++G(2df,pd) level (starting from B3LYP geometries optimization). The agreement between the PES experiments and OVGf calculations for INCO, ISCN, and ISeCN shows that the procedure used to synthesize these compounds is quite a good preparation method.

### PHOTOELECTRON SPECTROSCOPY AND CALCULATED STRUCTURE OF SO(N<sub>3</sub>)<sub>2</sub>, CH<sub>3</sub>C(O)X (X = NCO, NCS, N<sub>3</sub>) AND ClSO<sub>2</sub>Y (Y = NCO, N<sub>3</sub>)

Wang et al. [19] have reported vacuum preparation of the hitherto unknown thionyl azide SO(N<sub>3</sub>)<sub>2</sub> and its characterization by PES in combination with theoretical calculations. OVGf calculations using the 6-311++G(2df) basis set and frozen core MP2 optimized geometry of the *gauche* conformer have been performed on the ground and ionic states corresponding to ionization, with the electron being from different molecular orbitals with C<sub>1</sub> symmetry. The results were used to assign the PES bands.

Since there is no reported experimental geometry data, the structure of thionyl azide was optimized by both a frozen core MP2 and DFT (B3LYP) methods with the 6-31+G(d) basis set and three conformers were identified by both methods. The *cis*-conformer with C<sub>2v</sub> symmetry was shown to be a transition state by the frequency analysis (NIMAG=1). The other two minima of SO(N<sub>3</sub>)<sub>2</sub> have C<sub>1</sub> symmetry, with the *trans* conformer being 1.175 kcal/mol higher in energy than the *gauche* conformer at the CCSD/6-311G(d) level.

The assignment of the observed PE spectrum of SO(N<sub>3</sub>)<sub>2</sub> is supported by the OVGf calculation with 6-311++G(2df) basis set and on the basis of the Koopmans theorem [20]. Table 2 gives PES vertical ionization energies and ionization energies calculated by the OVGf method for the SO(N<sub>3</sub>)<sub>2</sub> molecule. The character of the ionized orbital corresponding to the PES band is also listed in Table 2.

The good agreement between the PES experiment and OVGf calculation shows that SO(N<sub>3</sub>)<sub>2</sub> has C<sub>1</sub> symmetry and the first ionization energy of 10.18 eV.

### PHOTOELECTRON SPECTRA AND ELECTRONIC STRUCTURES OF SOME CHLOROSULFONYL PSEUDOHALIDES

In order to obtain a deeper insight into the electronic structure of the molecules as well as to extract information on the change of molecular conformation accompanying the photo-ionization, the electronic structures of chlorosulfonyl pseudohalide ClSO<sub>2</sub>X (X = Cl, NCO, N<sub>3</sub>) was studied by PES in combination with OVGf calculation with 6-311++G(3df) basis sets [21]. The first vertical ionization potential for the three compounds is in agreement with the trend of the electronegativity of the three substituents: Cl > NCO > N<sub>3</sub>. The two structurally similar pseudohalogen substituents, NCO and N<sub>3</sub>, have different influence on the highest molecular occupied orbitals (HOMOs) of two corresponding compounds. The N<sub>3</sub> group in ClSO<sub>2</sub>N<sub>3</sub> has stronger interaction with the nonbonding electrons of chlorine than that of NCO in ClSO<sub>2</sub>NCO,

and this implies that the N<sub>3</sub> group is more pronounced in the first band of ClSO<sub>2</sub>N<sub>3</sub>. Meanwhile, the interaction between the pseudohalogen group and the chlorine “lone-pair” also affects the envelopes and width of the two dominant chlorine “lone-pair” ionization bands near 12.10 eV, compared to the first band of ClSO<sub>2</sub>Cl.

The two pseudohalogen substituents (NCO and N<sub>3</sub>) have different influence on the bond between sulfur and chlorine atoms in the chlorosulfonyl groups, although they have the same number of electrons. From the optimized geometries B3LYP/6-311++G(3*df*) level, the spatial distance between the N<sub>3</sub> group and chlorine in ClSO<sub>2</sub>N<sub>3</sub> is closer than the one between NCO and chlorine atom in ClSO<sub>2</sub>NCO. Consequently, the distance between sulfur and N<sub>3</sub> in ClSO<sub>2</sub>N<sub>3</sub> is evidently shorter than the sulfur-NCO bond length in ClSO<sub>2</sub>NCO, so the through-space *p*- $\pi$  interaction between chlorine *p*-orbital and the N<sub>3</sub> moiety is stronger than that between chlorine and the NCO moiety.

The geometric parameters of the energetically favored conformers of ClSO<sub>2</sub>NCO and ClSO<sub>2</sub>N<sub>3</sub>, compared with those in ClSO<sub>2</sub>Cl, indicate that the tetrahedron constructed by S–O atoms is more flat. It reflects the electron densities at these chemical bonds in the two compounds are more compact due to the weaker electron-withdraw effects of the NCO and N<sub>3</sub> groups. This trend was also revealed by the Mulliken density population at B3LYP/6-311++G(3*df*) level.

The AIM topological analysis [22] was also applied on ClSO<sub>2</sub>Cl, ClSO<sub>2</sub>NCO and ClSO<sub>2</sub>N<sub>3</sub> in order to describe their electronic structures in a quantitative way. Table 4 shows the selected chemical bond length,  $r_{S-X}$ , the distance between central S atom and the S–X BCP (bond critical point),  $r_{S-BCP}$ , the electron density at BCPs,  $\rho_b$ , and the Laplacian of electron density at BCPs,  $\nabla^2\rho_b$ . The increased  $\rho_{CP}$  of S–O in ClSO<sub>2</sub>NCO and ClSO<sub>2</sub>N<sub>3</sub>, as well as their corresponding large negative value of Laplacians of  $\rho_{CP}$ ,  $\nabla^2\rho$ , show that these bonds are polar, strongly covalent, electron-sharing bonds, while S–Cl bonds in these compounds exhibit weak ionic character with lower polarity.

As far as the S–X (X = Cl, NCO, N<sub>3</sub>) bonds are concerned in the latter two compounds, the S–N bonds between chlorosulfonyl and pseudohalogen groups are strong covalent interactions, that is, there are stronger *d*- $\pi$  interactions between NCO(N<sub>3</sub>) groups and sulfur atoms. Therefore, ClSO<sub>2</sub>NCO and ClSO<sub>2</sub>N<sub>3</sub> are distinguished from ClSO<sub>2</sub>Cl by their MO characters of frontier orbitals, which should be expected as the origins of the characteristic of their corresponding PE bands.

## PHOTOELECTRON SPECTRA AND ELECTRONIC PROPERTIES OF ACETYL PSEUDOHALIDES CH<sub>3</sub>C(O)X (X = NCO, NCS AND N<sub>3</sub>)

The HeI photoelectron spectra of acetyl pseudohalides, CH<sub>3</sub>C(O)X (X = NCO, NCS, N<sub>3</sub>) were studied by Zeng et al. [23]. After optimizations of the structures in order to find stable conformers at different levels of theory, a complete theoretical study involving the calculation of the ionization energies using OVGf function was performed. The geometrical parameters were obtained by HF, MP2/6-31+G(*d*), B3LYP/6-31+G(*d*) and B3LYP/6-311++G(*d,p*) approaches for the energetically favorable *cis* conformers (OVGF).

Acetyl pseudohalides can exist as a mixture of two planar conformers: *cis* and *trans* (Fig. 1) which have been located at the B3LYP/6-311++G(*d,p*) level of theory. The energy gaps between *cis* and *trans* conformers of the three molecules indicate that the *cis* conformer is lower in energy than the *trans* conformer at all levels of theory calculated for all the molecules studied, with the energy gaps being 2.36 kcal/mol and 1.23 kcal/mol (including ZPE) for CH<sub>3</sub>C(O)NCO and CH<sub>3</sub>C(O)NCS, respectively.

IR and Raman studies on acetyl isocyanate [24] and acetyl isothiocyanate [25] also indicate that the *cis* conformation is the preferred one in the gas phase. No experimental data on the conformation of acetyl azide was found but the experimental investigation on FC(O)N<sub>3</sub> [26] and methyl azidoformate [27] indicates that the *cis* conformer is also predominant in the gas phase in these both cases. Due to the similarity of the three triatomic pseudohalide moieties, the calculated structural parameters for three molecules do not differ drastically.

Although theoretical calculations (ROVGf/6-311++G(*d,p*)) for two isomers predict that the difference in the values of the IPs is negligible with respect to the experimental resolution, it was assumed that the *cis* isomer is the preferred conformer in the gas phase and that the spectra observed come from the energetically favorable isomer.

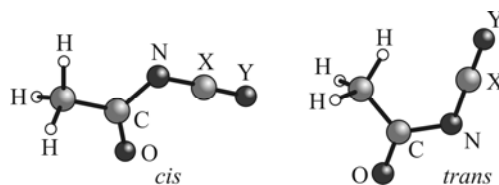


**Fig. 1.** Conformers of acetyl pseudohalides  $\text{CH}_3\text{C}(\text{O})\text{NXY}$  (e.g. for  $\text{CH}_3\text{C}(\text{O})\text{NCO}$   $\text{X} = \text{C}$  and  $\text{Y} = \text{O}$ ).

**TABLE 3.** Experimental Vertical Ionization Energies, IP, Computed Ionization Energies, Ev, (OVGF/6-311++G(*d,p*) calculations) and Molecular Orbital-Ionized Characters for *cis*- $\text{CH}_3\text{C}(\text{O})\text{NCO}$ <sup>a</sup>

Ev (eV)		MO	IP (eV)	Character	Ev (eV)		MO	IP (eV)	Character
<i>Cis</i>	<i>Trans</i>				<i>Cis</i>	<i>Trans</i>			
10.85	11.09	18 <i>a'</i>	10.72	$n_{\text{O}}, \pi'_{\text{NCO}}$	15.65	15.71	2 <i>a''</i>	15.39	$\pi_{\text{CH}_3}, \pi_{\text{NCO}}$
11.25	11.32	4 <i>a''</i>	11.33	$\pi_{\text{NCO}}, \pi_{\text{CO}}$	15.83	15.95	15 <i>a'</i>		$\sigma_{\text{C-O}}, \pi_{\text{NCO}}$
12.29	11.82	17 <i>a'</i>	12.48	$\pi'_{\text{NCO}}$	16.75	16.81	1 <i>a''</i>	16.52	$\pi_{\text{NCO}}$
13.76	13.95	3 <i>a''</i>	13.66	$\pi_{\text{CH}_3}, \pi_{\text{CO}}$	16.75	16.81	14 <i>a'</i>		
14.86	15.19	16 <i>a'</i>	14.55	$\pi'_{\text{CH}_3}$	17.41	17.56	13 <i>a'</i>	17.28	

<sup>a</sup>Taken from ref. [23].

**TABLE 4.** Electron Density Topology Properties of Selected Bonds in  $\text{ClSO}_2\text{Cl}$ ,  $\text{ClSO}_2\text{NCO}$ , and  $\text{ClSO}_2\text{N}_3$  Molecules<sup>a</sup>

Compound	Bond	$r_{\text{S-X}}$	$r_{\text{S-BCP}}$	$\rho_{\text{b}}$	$\nabla^2\rho_{\text{b}}$	Compound	Bond	$r_{\text{S-X}}$	$r_{\text{S-BCP}}$	$\rho_{\text{b}}$	$\nabla^2\rho_{\text{b}}$
$\text{ClSO}_2\text{Cl}$	S-Cl	2.073	1.001	0.1476	0.0247	$\text{ClSO}_2\text{N}_3$	S-Cl	2.060	0.982	0.1521	0.0310
	S-O	1.444	0.577	0.3106	-0.1781		S-N	1.688	0.738	0.2240	0.1338
$\text{ClSO}_2\text{NCO}$	S-Cl	2.054	0.979	0.1547	0.0340	S-O	1.417	0.568	0.3278	-0.2347	
	S-N	1.655	0.683	0.2280	0.1139						
	S-O	1.417	0.568	0.3287	-0.2316						

<sup>a</sup>Taken from ref. [21].

The interpretation of the PE spectra of the three molecules becomes straightforward while considering the similarities among the three quasi-linear triatomic pseudohalide groupings. Within the HeI energy region (21.2 eV), the non-bonding and bonding  $\pi$  level (of the originally linear moieties) will give rise to four IPs in the linear molecule, viz.  $a''$  (n.b.),  $a'$  (n.b.) and  $a''$  (b),  $a'$  (b). One group of orbitals with  $a'$  symmetry lies in the molecular plane, while the other group with  $a''$  symmetry belongs to orbitals perpendicular to the plane. These orbitals are partially localized on the pseudohalide carbonyl group and the pseudo- $\pi_{\text{CH}_3}$ . In the three acetyl pseudohalides, all  $\pi$  type bonds are in the  $C_s$  plane. The experimentally observed IP, calculated ionization energies at ROVGF/6-311CCG(*d,p*), molecular orbitals and molecular characters are summarized in Table 3.

On the whole, eight distinct ionization bands are observed in the region 10-18 eV. Three separate bands appear in the low ionization region (10-13 eV). The primary component for the first band is the oxygen lone-pair ( $n_{\text{O}}$ ) of the carbonyl group with  $a'$  symmetry.

The observed adiabatic and vertical ionization energies ( $I_{\text{a}} = I_{\text{v}} = 10.72$  eV) are in good agreement with the theoretically predicted (ROVGF/6-311CCG(*d,p*)) 10.85 eV for the energetically favorable *cis* isomer. The other two bands at 11.33 eV and 12.48 eV correspond to the first two PE bands of HNCO [28], the former is a result of the ionization of electrons on the orbital 4*a''*, composed by out-of-plane non-bonding  $\pi_{\text{NCO}}$ , while the latter is a result of ionization of

electrons on the orbital  $17a'$ , the main character being in-plane  $\pi'_{\text{NCO}}$ . The next two bands at 13.66 eV and 14.55 eV are characteristic bands for ionization electrons on the pseudo- $\pi_{\text{CH}_3}$  orbitals, also including in-plane and out-of-plane type.

The calculated vertical potentials for both bands are 13.76 eV and 14.86 eV, respectively; the contribution of  $\pi_{\text{CO}}$  should also be incorporated into the former ionization process. The sixth band from 14.80 eV to 16.0 eV is due to the overlap of out-of-plane  $2a''$   $\pi$  orbital ( $\pi_{\text{CH}_3}$ ,  $\pi_{\text{CO}}$  and  $\pi_{\text{NCO}}$ ) with the in-plane  $15a'$   $\sigma$  orbital ( $\sigma_{\text{CH}_3}$  and  $\sigma_{\text{CO}}$ ), the calculated ionization energies for both orbitals being 15.65 eV and 15.83 eV. The other bands in higher ionization energies range may be attributed to the ionization of inner orbitals of  $\text{CH}_3\text{-C(O)NCO}$ , which can not be assigned with absolute certainty.

The spectrum exhibits similarities in the region of 10-18 eV, due to the similarities among the three pseudohalide substituents: NCO, NCS and  $\text{N}_3$ . The first vertical ionization potentials for the three compounds are 10.72 eV, 9.75 eV, and 10.54 eV, respectively, that reflects the electronegativity of the three substituents:  $\text{NCO} > \text{N}_3 > \text{NCS}$ . The differences in vertical ionizations energies between the  $a'$  and  $a''$  components are consistent with a narrower angle C-N-X in  $\text{CH}_3\text{C(O)N}_3$  than that in  $\text{CH}_3\text{C(O)NCO}$  and  $\text{CH}_3\text{-C(O)NCS}$ . The three molecules retain planar structure after ionization.

## QUANTUM CHEMICAL STUDIES ON THE STRUCTURE OF VARIOUS PSEUDOHALIDES

Due to their structural diversity, inorganic pseudohalides can be bent or linear, have rigid or flexible frames, depending on the pseudohalide group and the nature of substituents. There is a number of possible pseudohalide isomers [29] with differing stabilities in the vapor phase. The substitution of the atoms of the pseudohalide group again provides various related molecules, sometimes with quite different properties. Veszprémi and coworkers performed *ab initio* calculations on a number of pseudohalide systems [30] and studied the large-amplitude bending motion by following the bending normal coordinate and calculating the optimum geometry with respect to all other coordinates [30c,f]. For beryllium pseudohalides [30g] new T-shaped isomers were found for thiocyanate and azide, where the beryllium atom is bonded to the two end atoms of the pseudohalide group, which is bent and forms a four membered ring with the substituent atom. The authors called these molecules “ $\pi$ -complexes” because they are stabilized by the interaction between the nonbonding orbitals of the pseudohalide  $\pi$ -system and the empty beryllium  $p$ -orbital of appropriate symmetry.

Furthermore, different pseudohalides were investigated by *ab initio* calculations (MP2/6-31G(*d,p*) level of theory) since they had been considered as promising species for  $\pi$ -complex formation. As an empty  $p$ -orbital of the ligand atom was believed to be important for the bonding in these molecules, the six first- and second-row atoms Li, Be, B, Na, Mg, and Al were tested as possible ligands. The  $\pi$ -complexes were shown to be stable equilibrium structures for different pseudohalides with  $-\text{NCO}$ ,  $-\text{NCS}$  and  $-\text{N}_3$  substituents.

The bonding is achieved between the empty  $p$ -orbital of the ligand atom and the  $\pi$ -system of the pseudohalide functional group. This is schematically shown in Figure 2 for  $\text{LiSCN}$ .

The  $\pi$ -complexes show an increasing tendency of formation in the series NCO,  $\text{N}_3$ , NCS and with the size of the substituent. The application of *ab initio* calculations made it possible to find that the cyclic form is between 12 kJ/mol and 16 kJ/mol more stable than the linear in  $\text{NaNCS}$ . Then, it appears likely that if the nitrogen atom in the pseudohalide group is replaced by the heavier phosphorus, the stability of the  $\pi$ -complex should increase.

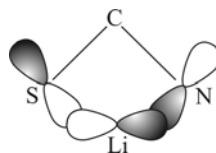


**Fig. 2.** Schematic representation of the proposed structure of  $\text{LiSCN}$ .

**TABLE 5.** Calculated Equilibrium Structure and Energies of Pseudohalide Derivatives of HCCNCO Isomers<sup>a,b</sup>

HCC–XYZ	HCC–NCO	HCC–OCN	HCC–CNO	HCC–ONC
H–C	1.060	1.060	1.061	1.060
C≡C	1.199	1.190	1.205	1.192
C–X	1.317	1.328	1.354	1.325
X–Y	1.202	1.308	1.164	1.349
Y–Z	1.165	1.151	1.201	1.173
HCC	178.7	179.0	180.0	179.7
CCX	176.1	175.5	180.0	175.3
CXY	146.7	117.8	180.0	113.3
XYZ	173.2	175.4	180.0	167.5
Total energy	–244.885309	–244.811438	–244.800762	–244.721239

<sup>a</sup>Taken from ref. [33].

<sup>b</sup>Bond lengths in Å, bond angles in degrees, total energies in a.u.; all of the electrons were included in the correlation energy calculations; calculated at B3LYP/6-311G(2d,2p).

In LiSCP and NaSCP, the linear isomers do not even appear on the potential energy surface. Even resorting to the choice of a larger basis set no linear form could be found and the optimum geometrical data for the cyclic isomer did not vary considerably using the MP2/6-311+G(*d*) and MP2/6-311+G(2*d*,*f*) levels of theory.

High-level *ab initio* calculations (full QCISD/6-311G(*d*) level) have demonstrated that the molecules LiPCS and NaPCS should only exist as tetraatomic rings in the vapor phase. As a result, they should be ideal candidates for providing proof for the existence of the  $\pi$ -complex form, which had been shown to be an isomer for a number of pseudohalides.

Experimental and theoretical study of the structure of NNO, HCNO, HNNN [31], HNCO and HNCS [32] was carried out in order to obtain information about their electronic structure and their interaction with He\*(2<sup>3</sup>S) and Li(2<sup>2</sup>S) atoms. Both experimental and calculated results indicate the existence of stable Li–M radicals (M = molecule of pseudohalogen). According to the calculations, HNCOLi and HNCSLi have a four-membered ring, where the lithium unpaired electron is delocalized on the HNCO and HNCS frame. Similar results were obtained with HNNN + Li and HCNO + Li. The thermodynamically most stable are systems that formed stable four-membered complexes with lithium atom. The unpaired electron of the lithium atom becomes completely delocalized on the CON or NNN frame, and the stabilization of this frame explains the large bonding energy of these  $\pi$ -type complexes.

The equilibrium geometries, stability and isomerization of the ethynyl pseudohalides, HCC–X (where X = –NCO, –OCN, –CNO, –ONC) have been investigated by *ab initio* MP2 and CCSD(T) as well as by B3LYP density functional methods using the 6-311G(2d,2p) basis set [33]. The existence of possible HCCNCO isomers was determined in order to obtain information about their relative thermodynamic stability. The calculated equilibrium structures of the thermodynamically most stable HCCNCO isomers indicate that there are five isomers; four of them are pseudohalide derivatives. Table 5 lists energies and geometries of these four isomers. It can be seen that ethynyl isocyanate, HCC–NCO, is the most stable molecule of all and it is planar.

The ethynyl group is close to linear with a CC triple bond in all derivatives (bond order: 2.9–3.0). Bond orders reveals  $\pi$ – $\pi$  interactions, since the unsaturated ethynyl group is connected to an unsaturated pseudohalide group and so the delocalization of  $\pi$ -electrons takes place over the entire molecular frames.

The calculated B3LYP and MP2 geometries are in agreement with each other. The experimental structure of HCC–NCO is in good agreement with calculated data (a comparison between experimental and calculated structure can be done only for this molecule since it is the only derivative with known experimental structure).

Minimum energy structures and their interconnecting transition states also were calculated and possible isomerization pathways were suggested. Three isomers, HCC–NCO, HCC–OCN and HCC–CNO, are kinetically stable

toward unimolecular isomerization or dissociation at room temperature (CCSD(T)/B3LYP calculations), and other isomers are unstable.

The gaps in the experimental data and varying levels of theoretical description make it necessary to use common basis and methodology that enable additional comparisons between molecules, both theoretical and experimental. Many experimental investigations use equilibrium structures as a model for their analysis, while calculated energy differences between conformers are also important in deconvoluting the spectra of mixtures of conformers, especially in experimental data. The equilibrium structures of various conformers of the azides, isocyanates and isothiocyanates with general formula  $\text{Me}_{3-n}\text{H}_n\text{W}-\text{N}=\text{X}=\text{Y}$  ( $\text{W} = \text{C}, \text{Si}$ ), together with a small number of their halogenated derivatives, have been studied by MP2 calculations under standard triple zeta valence + polarization basis set conditions [34]. It was an extensive theoretical study of these three series of compounds at the highest level of theory.

The CCSD(T) method, which is resource demanding even in smaller molecules, is likely to remain limited in choice, unless the analytic gradients procedure is both markedly increased in efficiency and run on parallel computers in highly parallel mode. On the other hand, the results show that it remains true that MP2 is currently a very practicable method, relatively non-demanding on computing resource, highly parallelized, uses analytic derivatives efficiently, and is eminently scaleable to larger atoms without difficulty. For most purposes, the principal features of importance both to structural and energetic studies can be obtained by MP2 methods, with considerable confidence. The most apparent limitation of MP2 is in accurate determination of low barriers to inversion in some of these compounds.

A comparison of the structures with theoretical studies including CCSD(T) results and with experimental spectral and diffraction data reveals that the MP2 and CCSD(T) results correlate strongly for a series of these molecules and the MP2 results for a wider group correlate closely with microwave and infrared spectra as well as with electron diffraction data. In contrast, the B3LYP method, with the same bases, whilst apparently providing reasonable structures, gives very poor rotation constants. However, the obtained results suggest that the spectra of ethyl isocyanate and silyl azide, as well as silyl isocyanate require an additional reinvestigation.

## PHOTOELECTRON SPECTROSCOPY AND STRUCTURE OF NITRILE OXIDES AND NITRILE SULFIDES

The first gas-phase generation of the unstable haloformonitrile oxide, BrCNO, was reported by Pasinszki and Westwood [35]. Apart from HeI photoelectron spectroscopy, HeI and  $\text{HL}_\alpha$  photoionization mass spectroscopy, and infrared spectroscopy studies of the species, its structure was pursued by quantum chemical calculations.

The calculated equilibrium geometry of BrCNO with standard 6-31G(*d*) basis set for the lighter atoms and one of [6*s*4*p*2*d*] quality for bromine changes markedly depending on the level of theory. The HF linear geometry could be due to neglect of electron correlation, but a linear geometry was also obtained at higher correlated levels, MP3, MP4SDQ, QCISD, and CCSD. The MP2, MP4SDTQ, QCISD(T) and CCSD(T) calculations, however, predict a structure bent at carbon with a smaller *trans* bend at nitrogen.

Similar dependence of the theoretical method on the equilibrium geometry has been found in the case of the parent nitrile oxide, fulminic acid (HCNO), a species routinely described as a quasi-linear molecule [36]. Even if the ambiguities between experiment and theory for HCNO and the similarities to the calculations on BrCNO could not have drawn any definitive conclusions on a linear or bent structure, the results obtained with the QCISD(T) or CCSD(T) methods suggest a linear or quasi-linear structure.

The HeI photoelectron and  $\text{HL}_{\alpha,\beta,\gamma}$  photoionization mass spectra (PIMS) confirm the identification of BrCNO. The infrared spectrum also indicates that the frame of the molecule must be linear or close to linear. By comparison of PE spectrum of BrCNO with the known PE spectra of HCNO [37] and BrCN [38, 39] as well as from the calculated IPs, the assignment is relatively straightforward (Table 6). The first three bands at 10.05 eV, 12.91 eV, and 15.80 eV were assigned

**TABLE 6.** Experimental and Calculated Ionization Potentials (eV) of BrCNO<sup>a</sup>

Exptl. IP <sup>b</sup>	Calc. <sup>c</sup>		Orbital symmetry and character	Exptl. IP <sup>b</sup>	Calc. <sup>c</sup>		Orbital symmetry and character
	MP3	QCISD			MP3	QCISD	
10.05	10.53 ( <i>a'</i> )	10.59 ( $\pi$ )	$\pi_{\text{nb}}$ (CNO)	15.80	18.33 ( <i>a'</i> )	18.36 ( $\pi$ )	$\pi_{\text{b}}$ (CNO)
	10.59 ( <i>a''</i> )		$\pi_{\text{nb}}$ (CNO)		18.69 ( <i>a''</i> )		$\pi_{\text{b}}$ (CNO)
12.91	13.92 ( <i>a'</i> )	14.08 ( $\pi$ )	$n_{\text{Br}}$	17.14	20.61 ( <i>a'</i> )	20.15 ( $\sigma$ )	$\sigma$ ( $n_{\text{O}}$ )
	13.98 ( <i>a''</i> )		$n_{\text{Br}}$	18.12	18.68 ( <i>a'</i> )	18.71 ( $\sigma$ )	$\sigma$ (C–Br)

<sup>a</sup>Taken from ref. [35].

<sup>b</sup>Vertical ionization potentials.

<sup>c</sup>Calculated via Koopman's theorem (unscaled).

to the two nonbonding  $\pi_{\text{nb}}$  (CNO), the two bromine lone pair  $n_{\text{Br}}$ , and the two bonding  $\pi_{\text{b}}$  (CNO) molecular orbitals, respectively. These orbitals, degenerate if the BrCNO chain is linear, split into *a'* and *a''* orbitals as the molecule bends at carbon. In BrCNO, no experimental splitting can be observed, although the first band is asymmetric.

One approach to assessing the linear/bent limit is to estimate the extent of  $\pi$  splitting at different fixed angles. The Br–C–N bond angle was set in 10° increments between 180° and 120°, and the rest of the geometry was optimized (MP2/6-31G(*d*)). As the experimental resolution was ~45 meV, a relatively small deviation from linearity (>12° in case of  $\pi_{\text{b}}$  (CNO) and >25° in the case of  $\pi_{\text{nb}}$  (CNO) or  $n_{\text{Br}}$ ) should manifest itself in observable splitting of the bands. However, this was not seen implying a linear or close to linear structure.

The terminal oxygen lone pair orbital leads to a strong sharp band in the spectrum of HCNO at 17.79 eV [37] and the band corresponding to the C–Br  $\sigma$  orbital appears in BrCN at 18.07 eV [39, 40]. Therefore, the last two bands in the spectrum at 17.14 eV and 18.12 eV were assigned to the  $n_{\text{O}}$  and C–Br  $\sigma$  orbitals, respectively.

The cyanogen di-N-oxide (ONCCNO), an unstable molecule, has been generated in high yield from *in situ* flow pyrolysis reactions of gaseous dichloroglyoxime or dibromofuroxan precursors and characterized by gas phase spectroscopy [41]. To complement the experimental studies, an assessment of the structure and bonding of ONCCNO was obtained from *ab initio* calculations at the HF, MP2, MP3 and MP4SDQ/6-31G\* levels of theory. The MP2 calculation gives a slightly bent equilibrium structure with a *trans*-bend at the C atoms ( $C_{2h}$  symmetry) and a barrier of 227 cm<sup>-1</sup> (0.65 kcal/mol), while the HF, MP3, and MP4SDQ calculations suggest a linear structure ( $D_{\sigma h}$ ) as preferable. On the basis of similar studies on the equilibrium structure of ClCNO and the flatness of the potential, the authors concluded that ONCCNO is most likely linear or quasi-linear.

The HeI photoelectron and HeI/HL <sub>$\alpha,\beta,\gamma$</sub>  photoionization mass spectra confirmed the identification of cyanogen di-N-oxide. Although low resolution, the infrared and photoelectron data indicate that the frame of the molecule must be linear or very close to linear.

The assignment of PE spectrum of ONCCNO in comparison with the known PE spectrum of HCNO [37] yields results relatively straightforward. The experimental and calculated IPs are presented in Table 7, the calculated (Koopmans') results for both linear and bent optimized structures. The first two bands at 9.95 eV and 12.02 eV were assigned to the  $\pi_{\text{nb}}$  (CNO) MOs, the  $2\pi_{\text{g}}$  and  $2\pi_{\text{u}}$  orbitals, destabilized and stabilized, respectively, from the mean location in HCNO, 10.83 eV. Since these bands are sharp and narrow, the authors concluded that the molecule must be linear or close to linear. The next bands at 15.8 eV ( $1\pi_{\text{g}}$ ) and 16.67 eV ( $1\pi_{\text{u}}$ ) were assigned to the bonding CNO  $\pi$  orbitals.

The last band between 17.8 eV and 18.4 eV (maximum around 18.1 eV) was assigned to the two nondegenerate oxygen terminal lone pair orbitals ( $7\sigma_{\text{g}}$  and  $7\sigma_{\text{u}}$ ). Such a terminal lone pair orbital ( $n_{\text{O}}$ ) leads to a strong sharp band in the individual PE spectra of HCNO [37] but experimentally no separation is observable in ONCCNO. No other bands were observed, in agreement with the calculations performed.

**TABLE 7.** Experimental and Calculated Ionization Potentials (eV) of ONCCNO<sup>a</sup>

Exp. IP <sup>b</sup>	Calc. MP3 <sup>c</sup>	Orbital symmetry and character	Exp. IP <sup>b</sup>	Calc. MP3 <sup>c</sup>	Orbital symmetry and character
9.95	10.66 (2 $\pi_g$ )	$\pi_{nb}$ (CNO)	17.8	20.89 (7 $\sigma_g$ )	$\sigma$ ( $n_O$ )
12.02	13.51 (2 $\pi_u$ )	$\pi_{nb}$ (CNO)		21.07 (6 $\sigma_u$ )	$\sigma$ ( $n_O$ )
15.8	19.27 (1 $\pi_g$ )	$\pi_b$ (CNO)	18.4	26.64 (6 $\sigma_g$ )	$\sigma$ (C–C)
16.67	19.99 (1 $\pi_u$ )	$\pi_b$ (CNO)			

<sup>a</sup>Taken from ref. [41].<sup>b</sup>Vertical ionization potentials.<sup>c</sup>Calculated via Koopman's theorem (unscaled).**TABLE 8.** Ionization Energies<sup>a</sup> (eV) of the XCNO Molecules

HCNO	ONCCNO	NCCNO	CICNO	BrCNO	H <sub>3</sub> CCNO	Orbital character	
10.83	9.95	11.28	10.28	10.05	9.92	$\pi_{nb}$ (CNO)	
	12.02					$\pi_{nb}$ (CNO)	
15.92	15.8	13.85	n.o. <sup>b</sup>	15.80	16.3	$\pi$ ( $n_X$ )	
		14.10				$\sigma$ ( $n_N$ )	
		17.08				$\pi_b$ (CNO)	
		16.67				$\pi_b$ (CNO)	
17.79	18.1	18.75	n.o. <sup>b</sup>	17.14	17.68	$\sigma$ (C–C)	
							$\sigma$ ( $n_O$ )
							$\sigma$ ( $n_O$ )
	18.1		n.o. <sup>b</sup>	18.12		$\sigma$ (C–Br)	

<sup>a</sup>Taken from ref. [43]; HCNO data from ref. [37].<sup>b</sup>Not observed; masked by HNCO.

HeI photoelectron and HeI and  $HL_{\alpha,\beta,\gamma}$  PIMS spectra were reported for unstable nitrile oxides XCNO ( $X = \text{ONC}^-$ ,  $\text{NC}^-$ ,  $\text{Cl}^-$ ,  $\text{Br}^-$  and  $\text{H}_3\text{C}^-$ ) generated in the gas phase from stable dihaloformaldoxime and disubstituted furoxan precursors [42]. Complete assessment of the the electronic structure of these molecules was made in the context of known data for the parent HCNO [37] molecule, thereby providing an assessment of substituent effects.

A general overview to the interpretation of the PE spectra (IEs provided in Table 8) shows that, except for ONCCNO which has connected CNO groups, a sharp band in the 9.9-11.3 eV region corresponds to the  $\pi_{nb}$  MO, and a broader band between 15.8 eV and 17.1 eV can be assigned to the  $\pi_b$  MO. The latter is then followed by a sharper band, 17.1-18.8 eV, attributable to the nonbonding terminal oxygen  $p\sigma$  orbital ( $n_O$ ). Interspersed between the  $\pi_{nb}$  and  $\pi_b$  orbitals are bands with principal localization on the substituent X, ranging from 12.9 eV (BrCNO) to 14.75 eV (H<sub>3</sub>CCNO).

The PE spectrum of ONCCNO is particularly interesting since in this case back-to-back –CNO groups split the  $\pi_{nb}$  orbital of the parent HCNO molecule into a  $\pi_g$  (9.95 eV) and  $\pi_u$  (12.02 eV) pair about the original position of 10.83 eV in HCNO. Likewise for the  $\pi_b$  orbital, the two bands are observed at 15.8 eV and 16.67 eV, the splitting centered marginally above 15.92 eV in HCNO. The  $\pi_{nb}$  separation is the highest of the two (2.07 eV) reflecting a large resonance interaction, whereas that of the  $\pi_b$  orbitals is much less at about 0.9 eV. The  $p\sigma$  orbitals in ONCCNO show essentially no separation, both components occurring in the band centered at 18.1 eV albeit still stabilized with respect to the corresponding band in HCNO.

The PE spectrum of NCCNO shows no real surprises and the PE spectra of nitrile oxides associated with halogen substituents place the ground ionic states at 10.28 eV (CICNO) and 10.05 eV (BrCNO), in both cases destabilized from the

corresponding value of 10.83 eV in HCNO. The structure of ClCNO, unobtainable from low-resolution IR, has been calculated with medium-scale *ab initio* calculations [43]. Although oscillations are observed in the MP $n$  series, the conclusion is that ClCNO must be a linear or quasi-linear species with a very low barrier to linearity. The spectrum of BrCNO shows the characteristic broad band corresponding to the  $\pi_b$  orbital at 15.80 eV. The two sharp peaks at 17.14 eV and 18.12 eV correspond to  $\Sigma$  cationic states; the first arises from the  $n_O$  orbital, the second belonging to  $\sigma(\text{C}-\text{Br})$ . This assignment was based on the trends observed in the calculations and were supported by OVGf calculations of the IEs.

H<sub>3</sub>CCNO is a symmetric top ( $C_{3v}$ ) with a linear heavy atom frame [42, 44]. In the PE spectrum obtained, the distinct  $\pi_{nb}$  and  $\sigma(n_O)$  bands appeared at 9.92 eV and 17.68 eV, respectively, the greater inductive effect manifested in the ca. 0.9 eV destabilization of the  $\pi_{nb}$  orbital. By analogy with similar methylcontaining species such as H<sub>3</sub>COCN [42], ionization from the  $e$  orbitals of the methyl group always comes between 14 and 16 eV, the broad band at 14.75 eV was assigned to  $e(\text{CH}_3)$ , with the broad feature with a maximum at 16.3 eV and a shoulder at 17.0 eV to the  $\pi_b$  and  $\sigma(\text{C}-\text{C})$  orbitals, respectively [42].

It is interesting to note that for the unstable methyl cyanate molecule, CH<sub>3</sub>OCN, [45] at MP2(fu11)/6-31G\*\* level of calculations the molecule has a bent structure with  $C_s$  symmetry. These calculations helped to support the spectrometric results of methyl cyanate and have indicated that two perspectives may be considered with regard to the electronic structure, a discrete ether-like formulation or a more delocalized  $-\text{OCN}$  model. The spectroscopy of methyl cyanate and the stable methyl isocyanate isomer showed that they are very different from each other, thus making it easy to distinguish between the two isomers. The most characteristic bands of CH<sub>3</sub>OCN for this purpose are those of  $n_N$  at 13.19 eV in the photoelectron spectrum, the CH<sub>3</sub><sup>+</sup> peak in the HL $_{\alpha,\beta,\gamma}$  PIMS, and  $\nu_s(\text{OCN})$  at 1112 cm<sup>-1</sup> in the infrared spectrum.

The trends obtained are important for investigating the electronic structures of these molecules. The spectra indicate that, for example, strong inductive effects occur upon substitution, and that ONCCNO is a highly coupled system, with the possibility of strong  $\pi$  interactions between the two CNO moieties. This suggests that the central C-C bond length is of some interest, since resonance structures can certainly be written involving single, double, or even triple bonds.

The generation of nitrile sulfides, XCNS (X = H, F, Cl, CN, CH<sub>3</sub>), in the gas phase by thermolizing 1,2,5-thiadiazoles was attempted, but in all cases the thiadiazoles were found to produce sulfur and the corresponding nitrile [46]. This prompted an investigation by computational methods for calculating the equilibrium geometries, stabilities, and decomposition mechanisms of the nitrile sulfides.

Due to the lack of experimental data, the reliability of the applied theoretical method cannot be tested by the usual procedure of comparing experiment and calculation. Because electron correlation and basis set effects are expected to be crucial as much as they are in the case of the nitrile oxides [44], the smallest and computationally most tractable derivative, HCNS, was selected as a test case with its geometry calculated at various levels of theory and basis set size.

The equilibrium structure of the parent nitrile sulfide, HCNS, was calculated at the HF, MP2, MP3, MP4, QCISD, QCISD(T), CCSD and CCSD(T) levels using standard 6-31G\*\*, 6-311G(2d,2p), 6-311+G(3df,3pd) or cc-pVTZ basis sets, and also using density functional theory in the form of Becke's three parameter exchange functional in combination with the Lee, Yang, and Parr correlation functional (B3LYP). The equilibrium geometries of the computationally larger derivatives, FCNS, ClCNS, NCCNS and CH<sub>3</sub>CNS, were calculated at the B3LYP/cc-pVTZ level.

Nevertheless, calculations on the nitrile sulfide structures are sensitive to electron correlation effects, and the description of these effects is of crucial importance, DFT can be a cost-effective approach for such molecules. Calculated B3LYP/cc-pVTZ geometry for the five molecules studied and the ionization potentials (IPs) are listed in Tables 9 and 10, respectively.

Calculations indicate that the molecules have linear heavy atom geometries; the exception is the fluoro derivative, which is bent with a calculated barrier to linearity of 889 m<sup>-1</sup>. The similarity to the nitrile oxides must be noted; FCNO is predicted to have a bent structure but all other substituted nitrile oxides can be described with a linear or quasi-linear frame [47]. The propensity for bending in XCNO species increases with the increase in electronegativity of the substituent attached

**TABLE 9.** Calculated<sup>a</sup> Equilibrium Structure of Nitrile Sulfides, XCNS (X = H, F, Cl, NC, and CH<sub>3</sub>)<sup>b</sup>

	HCNS	FCNS	CICNS	NCCNS	H <sub>3</sub> CCNS
X–C	1.061	1.296	1.625	1.349	1.449
C–N	1.160	1.186	1.163	1.171	1.159
N–S	1.603	1.589	1.609	1.577	1.619
N–C				1.161	
C–H					1.092
XCN	180.0	139.5	180.0	180.0	180.0
CNS	180.0	169.2	180.0	180.0	180.0
NCC				180.0	
HCC					110.5
Total energy	–491.65340	–590.88996	–951.27123	–583.92544	–530.99799

<sup>a</sup>Taken from ref. [46].<sup>b</sup>Calculated at the B3-LYP/cc-pVTZ level. Bond angles in degrees, bond lengths in angstroms, total energies in a.u.**TABLE 10.** Calculated<sup>a</sup> Vertical Ionization Potentials (in eV) of Nitrile Sulfides, XCNS<sup>b</sup>

HCNS	FCNS	CICNS	NCCNS	H <sub>3</sub> CCNS	MO character
8.98 $\pi$	9.27 $a''$ 9.52 $a'$	8.67 $\pi$	9.66 $\pi$	8.37 $e$	$\pi_{nb}$ (CNS)
14.86 $\pi$	13.92 $a'$ 14.33 $a''$	13.46 $\pi$	13.20 $\pi$	14.00 $e$	$\pi_b$ (CNS)
15.72 $\sigma$	16.30 $a'$	15.57 $\sigma$ 15.69 $\pi$	13.97 $\sigma$ 15.74 $\pi$ 16.65 $\sigma$	15.12 $a_1$ 16.35 $e$ 17.35 $a_1$	$n_N$ $\pi$ (NC) $n_S$ (S lone pair) $n_{Cl}$ CH <sub>3</sub> CH <sub>3</sub> C–Cl
		18.75 $\sigma$			

<sup>a</sup>Calculated using the ROVGF/cc-pVTZ method at the B3LYP/cc-pVTZ geometries.<sup>b</sup>Taken from ref. [46].

to the –CNO group and the increase in the C=N bond length shows the same trend [47]. This can be seen in Table 2 for nitrile sulfides as well.

## CONCLUSIONS

Due to their varied structure, stability, and reactivity, pseudohalides continuously attract attention of researchers in various fields of chemistry. They are unsaturated and usually exhibit large amplitude deformations, thus the description of their behavior requires the application of acceptable and proper theoretical methods.

In this review we discussed the progress that has been made mainly in the two past decades. While many successful preparations and spectroscopic characterizations of pseudohalides have been considered, we have concentrated our attention on quantum chemical studies using DFT or *ab initio* methods in this field. Emphasis has been given to describing the physical and chemical properties of pseudohalides that give more useful information related to the chemical bond.

The research reviewed in this paper shows the remarkable progress which has been made in the last years toward gaining insight into the chemical bonding in pseudohalide-containing compounds.

Financial support from SECYT-UNNE UNLP is gratefully acknowledged. A.H.J. is a member of the Research Career, CIC, Buenos Aires, and E.A.C. and N.B.O. are members of the Research Career of CONICET, Argentina. Both reviewers are thanked for their comments which greatly improved the manuscript.

## REFERENCES

1. E. Hückel, *Z. Phys.*, **70**, 204 (1931).
2. J. A. Berson, *Angew. Chem. Int. Ed.*, **35**, 2750 (1996).
3. L. Pauling, *The Nature of the Chemical Bond*, 3rd ed.; Cornell University Press, Ithaca, New York (1960), p. 286.
4. a) *Density Functional Methods in Chemistry*; J. Labanowski and J. Andzelm (eds.), Springer-Verlag: Heidelberg (1991); b) *Density Functional Theory of Atoms and Molecules*, R. G. Parr and W. Yang (eds.), Oxford University Press, New York (1988).
5. *IUPAC Compendium of Chemical Terminology*, **67**, 1361 (1995).
6. L. Birkenbach and K. Kellermann, *Ber. Dtsch. Chem. Ges.*, **58B**, 786 (1925).
7. F. Holleman, N. Wiberg, and E. Wiberg, *Lehrbuch der Anorganischen Chemie*, 101st ed., Walter de Gruyter, Berlin (1995).
8. a) M. Ghedini, D. Pucci, E. Cesarotti, et al., *Chem. Mater.*, **5**, 883 (1993); b) M. Ghedini, S. Morrone, O. Francescangeli, and R. Bartolino, *Chem. Mater.*, **6**, 1971 (1994); c) H. Chowdhury, S. H. Rahaman, R. Ghosh, et al., *J. Mol. Struct.*, **826**, 170 (2007).
9. a) K. Nakamoto, *Infrared and Raman Spectra of Inorganic and Coordination Compounds, Part B, Applications in Coordination, Organometallic, and Bioinorganic Chemistry*, Wiley, New York (1997); b) O. H. Ellestad, P. Klæboe, E. E. Tucker, and J. Songstad, *Acta Chem. Scand.*, **26**, 1721 (1972).
10. a) M. A. S. Goher and F. A. Mautner, *J. Chem. Soc. Dalton Trans.*, 1923 (1999); b) C. Diaz, J. Ribas, M. S. El Fallah, et al., *Inorg. Chim. Acta.*, **312**, 1 (2001); c) R. Ghosh, S. H. Rahaman, Ch. Lin, et al., *Polyhedron*, **25**, 3104 (2006).
11. a) A. D. Ryabov, *Synthesis*, 233 (1985); b) M. Pfeffer, J. P. Sutter, A. DeCian, and J. Fisher, *Inorg. Chim. Acta.*, **220**, 115 (1994); c) F. Maassarani, M. Pfeffer, J. Spencer, and E. Wehman, *J. Organometal Chem.*, **466**, 265 (1994).
12. a) J. D. Higgis, *J. Inorg. Biochem.*, **49**, 149 (1993); b) C. Navarro-Ranninger, I. Lopez-Solera, J. M. Perez, et al., *Appl. Organomet. Chem.*, **7**, 57 (1993).
13. a) T. J. Mizoguchi and S. J. Lippard, *Inorg. Chem.*, **36**, 4526 (1997); b) S. S. Lemos, M. A. Camargo, Z. Z. Cardoso, et al., *Polyhedron*, **20**, 849 (2001); c) D. P. Kessissoglou, J. J. Bodwin, J. Kampf, et al., *Inorg. Chim. Acta.*, **331**, 73 (2002); d) R. B. Bedford, C. S. J. Cazin, S. J. Coles, et al., *Organometallics*, **22**, 987 (2003); e) R. B. Bedford, C. S. J. Cazin, S. J. Coles, et al., *J. Chem. Soc., Dalton Trans.*, 3350 (2003); f) I. J. S. Fairlamb, A. R. Kapdi, J. M. Lynam, et al., *Tetrahedron*, **60**, 5711 (2004); g) J. L. Serrano, I. J. S. Fairlamb; G. Sánchez, et al., *Eur. J. Inorg. Chem.*, 2706 (2004); h) J. Honzík, M. Erben, I. Císařová, and J. Vinklár, *Inorg. Chim. Acta.*, **358**, 814 (2005); i) S. H. Rahaman, H. Chowdhury, D. Bose, et al., *Polyhedron*, **24**, 1755 (2005); j) T. M. Klapötke, B. Krumm, and I. Schwab, *Phosphorus, Sulfur, and Silicon and the Related Elements*, **180**, issue 3/4, 957 (2005); k) M. L. Dias, L. P. Da Silva, G. L. Crossetti, et al., *J. Polym. Sci., Part A, Polym. Chem.*, **44**, No. 1, 458 (2006); l) W. Chen, M. S. Wang, X. Liu, et al., *Cryst. Growth Des.*, **6**, No. 10, 2289 (2006).
14. a) M. I. Al-Joboury and D. W. Turner, *J. Chem. Phys.*, **37**, 3007 (1962); b) F. I. Vilesov, B. L. Kurbatov, and A. N. Terenin, *Sov. Phys. Dokl.*, **6**, 490 (1961); c) D. W. Turner, C. Baker, A. D. Baker, and C. R. Brundle, *Molecular Photoelectron Spectroscopy*, Wiley Interscience, London (1970).
15. a) D. C. Frost, C. B. Macdonald, C. A. McDowell, and P. C. Westwood, *Chem. Phys.*, **47**, No. 1, 111 (1980); b) D. C. Frost, C. B. Macdonald, C. A. McDowell, and N. P. C. Westwood, *J. Am. Chem. Soc.*, **103**, 4423 (1981).
16. H. Leung, R. J. Suffolk, and J. D. Watts, *Chem. Phys.*, **109**, 289 (1986).
17. H. J. Che, H. M. Bi, Y. L. Zeng, et al., *Chem. Phys. Chem.*, **3**, 300 (2003).

18. Y. Li, Z. Qiao, Q. Sun, et al., *Inorg. Chem.*, **42**, 8446 (2003).
19. X. Zeng, F. Liu, Q. Sun, et al., *ibid.*, **43**, 4799 (2004).
20. T. Koopmans, *Physica*, **1**, 104 (1934).
21. L. Fengyi, Z. Xiaoqing, W. Weigang, et al., *Spectrochim. Acta A*, **63**, 111 (2006).
22. R. F. W. Bader, *Atoms in Molecules. A Quantum Theory*, Clarendon, Oxford (1990).
23. X. Zeng, L. Yao, M. Ge, and D. Wang, *J. Mol. Struct.*, **789**, 92 (2006).
24. a) W. J. Balfour, S. G. Fougère, D. Klapstein, and W. M. Nau, *ibid.*, **299**, 21 (1993); b) K. A. Krutules, J. F. Sullivan, G. A. Guirgis, et al., *ibid.*, **293**, 23 (1993).
25. a) J. R. Durig, G. A. Guirgis, and K. A. Krutules, *ibid.*, **328**, 97 (1994); b) N. L. Campbell, C. J. Gillis, D. Klapstein, and W. M. Nau, *Spectrochim. Acta, Part A*, **51**, 787 (1995).
26. H. G. Mack, C. O. D. Védova, and H. Willner, *J. Mol. Struct.*, **291**, 197 (1993).
27. R. K. Kakar, C. R. Quade, W. Lwowski, and R. E. Wilde, *J. Chem. Phys.*, **72**, 4123 (1980).
28. S. Cradock, E. A. V. Ebsworth, and J. D. Murdoch, *J. Chem. Soc., Faraday Trans.*, **68**, 86 (1972).
29. a) D. Poppinger, L. Radom, and J. A. Pople, *J. Am. Chem. Soc.*, **99**, 7806 (1977); b) D. Poppinger and L. Radom, *ibid.*, **100**, 3674 (1978).
30. a) T. Veszprémi, T. Pasinszki, and M. J. Fehér, *Chem. Soc., Faraday Trans.*, **87**, 3805 (1991); b) T. Pasinszki, T. Veszprémi, and M. Fehér, *Chem. Phys. Lett.*, **189**, 245 (1992); c) M. Fehér, T. Pasinszki, T. Veszprémi, *J. Phys. Chem.*, **97**, 1538 (1993); d) M. Fehér, T. Pasinszki, and T. Veszprémi, *J. Am. Chem. Soc.*, **115**, 1500 (1993); e) M. Fehér, T. Pasinszki, and T. Veszprémi, *Chem. Phys. Lett.*, **205**, 123 (1993); f) T. Pasinszki, T. Veszprémi, M. Fehér, *J. Mol. Struct. (THEOCHEM)*, **331**, 289 (1995); g) T. Pasinszki, T. Veszprémi, and M. Fehér, *Chem. Phys. Lett.*, **215**, 395 (1993); h) T. Veszprémi and T. Pasinszki, *Inorg. Chem.*, **35**, 2132 (1996).
31. T. Pasinszki, N. Kishimoto, and K. Ohno, *J. Phys. Chem.*, **A103**, 6746 (1999).
32. T. Pasinszki, N. Kishimoto, and K. Ohno, *ibid.*, 9195.
33. T. Pasinski and B. Havasi, *Phys. Chem. Chem. Phys.*, **5**, 259 (2003).
34. M. H. Palmer and A. D. Nelson, *J. Mol. Struct.*, **689**, 161 (2004).
35. T. Pasinszki and N. P. C. Westwood, *J. Phys. Chem.*, **99**, 6401-6409 (1995).
36. N. Pinnavaia, M. J. Bramley, M.-D. Su, et al., *Mol. Phys.*, **78**, 319 (1993).
37. J. Bastide and J. P. Maier, *Chem. Phys.*, **12**, 177 (1976).
38. R. F. Lake and H. Thompson, *Proc. Roy. Soc. London A*, **317**, 187 (1970).
39. E. Heilbronner, V. Homung, and K. A. Muszkat, *Helv. Chim. Acta*, **53**, 347 (1970).
40. R. F. Lake and H. Thompson, *Proc. Roy. Soc. London A*, **317**, 187 (1970).
41. T. Pasinszki and N. P. C. Westwood, *J. Am. Chem. Soc.*, **117**, 8425 (1995).
42. T. Pasinszki and N. P. C. Westwood, *J. El. Spectr. Rel. Phenom.*, **97**, 15 (1998).
43. T. Pasinszki and N. P. C. Westwood, *J. Phys. Chem. A*, **102**, 4939 (1998).
44. T. Pasinszki and N. P. C. Westwood, *ibid.*, **105**, 1244 (2001).
45. T. Pasinszki and N. P. C. Westwood, *J. Phys. Chem.*, **99**, 1649 (1995).
46. T. Pasinszki, T. Kárpáti, and N. P. C. Westwood, *J. Phys. Chem. A*, **105**, 6258 (2001).
47. T. Pasinszki and N. P. C. Westwood, *J. Mol. Struct.*, **408/409**, 161 (1997).